ACS APPLIED MATERIALS & INTERFACES

Research Article

www.acsami.org

Formation of Liquid-Crystalline Structures in the Bile Salt−Chitosan System and Triggered Release from Lamellar Phase Bile Salt−Chitosan Capsules

Kristian J. Tangso,[†] Seth Lindberg,[‡] Patrick G. Hartley,[§] Robert Knott,[∥] Patrick Spicer,[⊥] and Ben J. Boyd*[,†]

[†]Drug Delivery, Disposition and Dynamics, Monash Institute of Pharmaceutical Sciences, Monash University (Parkville Campus), 381 Royal Parade, Parkville, Victoria 3052, Australia

[‡]The Procter and Gamble Company, Corporate Engineering Technical Laboratories Building, Cincinnati, Ohio 45069, United States

[§]Commonwealth Scientific and Industrial Research Organization, Bag 10, Clayton South, VIC 3169, Australia

[∥]Bragg Institute, Australian Nuclear Science and Technology Organization, Menai, NSW 2234, Australia

[⊥]School of Chemical Engineering, University of New South Wales, Sydney, NSW 2052, Australia

Supporting Information

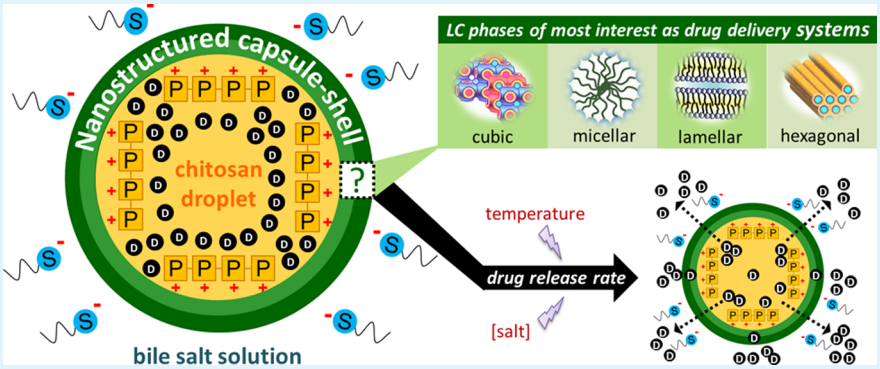

ABSTRACT: Nanostructured capsules comprised of the anionic bile salt, sodium taurodeoxycholate (STDC), and the biocompatible cationic polymer, chitosan, were prepared to assess their potential as novel tailored release nanomaterials. For comparison, a previously studied system, sodium dodecyl sulfate (SDS), and polydiallyldimethylammonium chloride (polyDADMAC) was also investigated. Crossed-polarizing light microscopy (CPLM) and small-angle X-ray scattering (SAXS) identified the presence of lamellar and hexagonal phase at the surfactant−polymer interface of the respective systems. The hydrophobic and electrostatic interactions between the oppositely charged components were studied by varying temperature and salt concentration, respectively, and were found to influence the liquid-crystalline nanostructure formed. The hexagonal phase persisted at high temperatures, however the lamellar phase structure was lost above ca. 45 °C. Both mesophases were found to dissociate upon addition of 4% NaCl solution. The rate of release of the model hydrophilic drug, Rhodamine B (RhB), from the lamellar phase significantly increased in response to changes in the solution conditions studied, suggesting that modulating the drug release from these bile salt−chitosan capsules is readily achieved. In contrast, release from the hexagonal phase capsules had no appreciable response to the stimuli applied. These findings provide a platform for these oppositely charged surfactant and polymer systems to function as stimuli-responsive or sustained-release drug delivery systems.

KEYWORDS: *chitosan, bile salt, thermoresponsive liquid crystals, release studies, SAXS, lamellar phase*

1. INTRODUCTION

Formation of liquid-crystalline phases or "mesophases" in mixtures of oppositely charged surfactant and polymer solutions has been known since the late 1970s.[1,2] There is increasing interest in these particular materials, as they offer great versatility in structure manipulation over oppositely charged polymer-based drug delivery systems such as layer-by-layer (LbL) engineered capsules.[3,4] Complex nanostructures have potential applications in the cosmetic,[5] food, consumer, and pharmaceutical industries.[6−8]

Liquid-crystalline systems are excellent candidates as drug carriers for their ability to solubilize therapeutics with a diversity of physicochemical properties. It is also well-known

Received: April 11, 2014
Accepted: July 22, 2014

   dx.doi.org/10.1021/am502192t | ACS Appl. Mater. Interfaces XXXX, XXX, XXX−XXX

that the liquid-crystalline nanostructure controls the drug release rate from these matrices,[9−11] therefore it is advantageous to have control over which mesophase is formed. This may be achieved by introducing variables that can modulate the electrostatic and/or hydrophobic interactions between the oppositely charged species, which in turn influences their geometric packing that dictates the liquid-crystalline phase formed. These experimental parameters include the surfactant-to-polymer molar charge ratio,[12−14] surfactant chain length,[15−17] polymer molecular weight,[18,19] and charge density,[20−22] temperature,[7,23−27] pH,[28] and ionic strength.[29−31]

There has been much research into cationic lipids and DNA for use in gene therapy;[31−33] however, studies on biocompatible anionic surfactant and cationic polymer systems have received little attention. Bile acids, or bile salts, are biological anionic amphiphiles that exhibit great solubilization capacity for lipids, such as lecithin and cholesterol,[34] through formation of micelles at dilute conditions. At higher concentrations, bile salts can form more highly ordered liquid-crystalline phases, such as hexagonal phase.[35] Chitosan is a cationic polysaccharide produced from the deacetylation of chitin, a natural component abundantly sourced from the shells of crustaceans. Its biocompatibility, biodegradability, low toxicity and mucoadhesive properties enable chitosan to be used in skin products, cosmetic and biomedical materials, and has potential to function as a novel carrier of drugs for oral and intravenous administration.[36] Drug delivery via the buccal route is advantageous as it provides a rich blood supply, good accessibility for self-medication, patient compliance, and safeness, and most importantly bypasses the hepatic first-pass metabolism and degradation within the gastrointestinal tract. However, this route of drug administration also possesses a few limitations, including poor permeability of high-molecular-weight molecules,[37,38] requiring penetration enhancers that tend to cause mucosal damage, as well as needing protection from enzymes introduced within the saliva. Systems comprising a combination of both bile salt and chitosan have recently become a growing field of interest (chemical structures shown in Figure 1).

The previously studied system comprising the anionic surfactant sodium dodecyl sulfate (SDS), and the cationic polymer polydiallyldimethylammonium chloride (polyDADMAC), are industrially relevant materials that were chosen in these studies as a known comparative system (chemical structures shown in Figure 1). Independently, SDS and polyDADMAC have been used as detergents in cleaning products and as coagulants in wastewater treatment, respectively. Synergistically, they encompass the commonly exploited ingredients in hair products and are known to form hexagonal phases at certain mole ratios.[13,17,25,39,40]

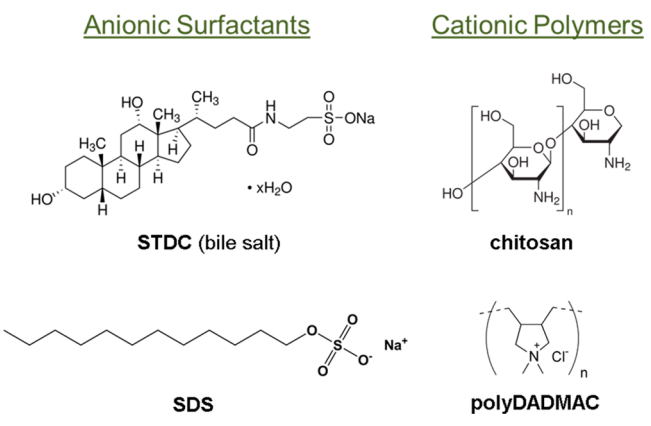

Figure 1. Chemical structures of the anionic surfactants, bile salt (sodium taurodeoxycholate, STDC), and sodium dodecyl sulfate (SDS), and the cationic polymers, chitosan, and polydiallyldimethylammonium chloride (polyDADMAC).

This paper aims to (i) identify the liquid-crystalline phases formed at the interface between contacted surfactant and polymer solutions,[41] study the growth and development of nanostructures across this interface with varying polymer concentration, (iii) probe the strength of hydrophobic and electrostatic interactions between moieties by examining how the nanostructures are influenced by changes in solution temperature and salt concentration, (iv) determine the diffusion coefficient of a model hydrophilic drug from macro-sized capsules possessing nanostructured "shells" at different solution conditions. The phase behavior of the bile salt−chitosan system is contrasted to that of the SDS−polyDADMAC system. Gaining a further understanding of how the structural attributes of these oppositely charged surfactant and polymer moieties can be manipulated would assist in formulating a novel and interesting route for responsive liquid-crystalline nanomaterials.[42]

2. EXPERIMENTAL SECTION

2.1. Materials. Sodium taurodeoxycholate hydrate (STDC, BioXtra, ≥97% (TLC), chitosan- low molecular weight (≥75.0% deacetylation), Rhodamine B (RhB, dye content 90%), acetic acid (ReagentPlus, ≥ 99%), and sodium dodecyl sulfate (SDS, BioXtra, ≥99.0%) were purchased from Sigma-Aldrich (Sydney, Australia). Dioleylphosphatidyl choline (DOPC, >94%) was obtained from Trapeze Associates Pty Ltd. (Victoria, Australia), and polydiallyldimethylammonium chloride (polyDADMAC, commercial name: Merquat 100, molecular weight: 1.5×10^5 g/mol) was sourced from Nalco Company (Naperville, IL, USA). These materials were used without further purification. Milli-Q grade water purified through a Milli-pore system was used throughout this study.

2.2. Characterization of Liquid-Crystalline Nanostructures. *2.2.1. Sample Preparation.* All stock solutions were prepared by weight. Chitosan is known to be readily soluble in acidic conditions where it predominantly exists in its protonated form. For this reason and for the interest of the studies presented in this paper, stock solutions of bile salt and chitosan were both prepared in 10% (v/v) acetic acid; where the solution pH was not adjusted. The liquid-crystalline structure formed in systems comprised of fixed bile salt-to-chitosan composition was not influenced by pH (see Figure S1 in the Supporting Information). Bile salt concentration was held constant throughout the studies at 30 wt % STDC. Solutions of chitosan were prepared at 1, 2, 3, 4, 5, and 6 wt % to explore how the apparent viscosity of the polymer solution influences the kinetics of structure formation across bile salt−chitosan interfaces.

To study the dynamics of structure formation between oppositely charged surfactant and polymer solutions, we created a "neat" well-defined interface between the two components. This was achieved by loading the bottom half of an open-ended VitroCom borosilicate "flat cell" (dimensions: 0.4 × 8.0 × 50 mm) with polymer solution via capillary action, and the slow addition/layering of surfactant solution from the top of the cell opening; then sealing both ends with parafilm (Scheme 1). The location of the initial interface formed was marked on the cell as a guide to monitoring the development of structure formation across the bile salt−chitosan interface over time; the distance being referred to as the "distance from origin" (Figure 2).

The effect of salt concentration on the liquid-crystalline phase formed was studied slightly differently, using a circular rather than a linear interface. This enabled replacement of the 30 wt % bile salt solution that surrounded a disc of 4 wt % chitosan solution (delivered

Scheme 1. Sample Preparation in Flat Cells for Studying Structural Behavior at Surfactant−Polymer Interfaces

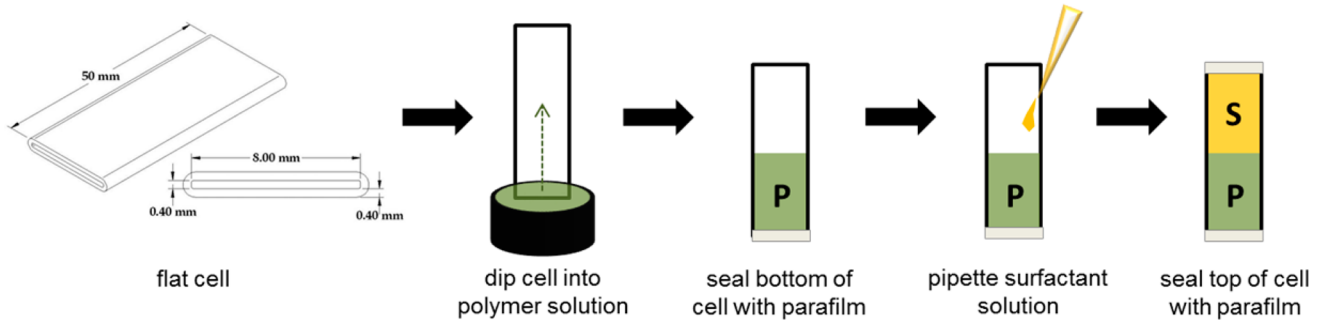

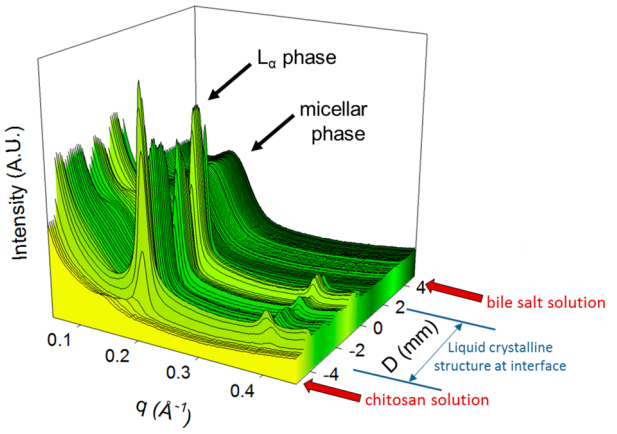

Figure 2. SAXS scattering profiles as a function of "distance from origin", *D*, obtained during a spatial line scan, across a system comprised of 4 wt % chitosan (bottom) and 30 wt % STDC solution,[61] where the lamellar structure was allowed to develop over 1 week from when the initial surfactant−polymer interface was created (0 mm).

into the flat cell via a 27G syringe), with 4% NaCl solution. This arbitrary salt concentration was chosen as it was in excess of the theoretical amount of salt required to force the SDS−polyDADMAC equilibrium reaction toward the reactants in order to induce the dissociation of the nanostructure formed in the system comprised of 20 wt % SDS and 20 wt % polyDADMAC solution.

2.2.2. Crossed-Polarizing Light Microscopy (CPLM) and Hot Stage Microscopy (HSM). CPLM was used as a prescreening step to indicate the presence and growth of liquid-crystalline phases formed at the bile salt−chitosan interfaces. Images of samples loaded in flat cells were taken at various time intervals using a Nikon ECLIPSE Ni−U upright microscope fitted with crossed-polarizing filters and a DS-U3 digital camera control unit (Nikon, Japan). Isotropic phases, such as cubic and micellar phases, appear dark under crossed-polarized light, whereas the anisotropic structures (hexagonal and lamellar phases) exhibit birefringence (appear bright under crossed-polarizers) and their characteristic textures can be observed.[43]

To optically examine the effect of salt on the stability of existing liquid-crystalline phase(s) formed between the oppositely charged solutions, images were taken of the samples before and after addition of 4% NaCl solution.

Hot stage microscopy was employed to probe any changes to the liquid-crystalline structure(s) in response to heating. Samples loaded in flat cells were gradually heated at a rate of 5 °C/min from 25 to 60 °C using a Mettler Toledo FP82HT hot stage fitted with a FP90 Central Processor temperature controller and viewed under the microscope.

2.2.3. Small-Angle X-ray Scattering (SAXS). To determine the structural attributes of phases formed at the bile salt−chitosan interfaces, two different SAXS instruments were used. For equilibrium temperature scans and pH studies, a Bruker lab source was utilized, whereas for spatial line scans and kinetic studies, the SAXS/WAXS beamlime at the Australian Synchrotron was used.[44] Both are described in more detail below.

As a complementary technique to hot stage microscopy, benchtop SAXS at the Bragg Institute at the Australian Nuclear Science and Technology Organisation was used in order to verify the structural integrity of respective nanostructures formed in mixtures of bile salt−chitosan (30 wt %: 4 wt %) and SDS−polyDADMAC (20 wt %: 20 wt %) in response to heating. Sample mixtures were prepared by dropwise addition of surfactant solution (500 μL) into polymer solution (500 μL), vortex mixed, then left to equilibrate on rollers in an incubator oven set at ca. 37 °C for at least 1 week prior to analysis. Samples were packed into quartz glass capillaries (Capillary Tube Supplies Ltd., Germany) with a path length of 2.0 mm, sealed with wax and then inserted into a thermostated metal heating block controlled by a Peltier system accurate to ±0.1 °C. The samples were introduced to the beamline of a Bruker Nanostar SAXS camera, with pinhole collimation for point focus geometry. The instrument source was a copper rotating anode (0.3 m filament) operating at 45 kV and 110 mA, fitted with cross-coupled Göbel mirrors, resulting in CuKα radiation wavelength 1.54 Å. The SAXS camera was fitted with a Hi-star 2D detector (effective pixel size 100 μm) which was located 650 mm from the sample to provide a q-range of 0.008−0.3910 Å^{-1}. Scattering patterns were collected over 30 min under vacuum to minimize air scatter. Samples were heated stepwise from 25 to 80 °C at 5 °C increments.

Samples prepared in flat cells were introduced into the SAXS/WAXS beamline at the Australian Synchrotron and a line scan conducted from the bottom (bulk polymer solution), through the surfactant−polymer interface to the top of the sample (bulk surfactant solution) at a spatial resolution of 100 μm increments (q-range of 0.0160−1.0432 Å^{-1}). At each position, 2D SAXS patterns were collected with 1 s acquisition using a 1 M Pilatus detector (active area 169 × 179 mm^2 with a pixel size of 172 μm.)

The computer software ScatterBrain Analysis was used to reduce the 2D scattering patterns to the 1D scattering function $I(q)$. The d-spacing of the liquid-crystalline lattice is derived from Bragg's law ($2d\sin\theta = n\lambda$, where n is an integer, λ is the wavelength, θ is the scattering angle). Because the scattering profiles of various liquid-crystalline phases have been well-characterized using SAXS,[45] observing the difference in relative positions of the Bragg peaks, correlated by the Miller indices of known phases, allows the recognition of nanostructure(s) that exist in samples of interest. The lamellar (L_α) phase can be identified by Bragg reflections that are equidistant, whereas the hexagonal phase can be identified by the Bragg reflections at spacing ratios $1:\sqrt{3}:\sqrt{4}$, etc. The micellar phase is identified by a single characteristic broad peak. The absolute location of the peaks allow for the calculation of the mean lattice parameter, a, of the matrices, from the corresponding interplanar distance, d ($d = 2\pi/q$)), using the appropriate scattering law for the phase structure.[45] For lamellar phases, $a = d$, whereas for the hexagonal phases, $a = 4d/3(h^2 + k^2)^{1/2}$, where h and k are the Miller indices for the particular structure present.[45]

dx.doi.org/10.1021/am502192t | ACS Appl. Mater. Interfaces XXXX, XXX, XXX−XXX

2.2.4. In Vitro Release Studies. Proof of concept release studies were conducted in triplicate with the purpose of determining the diffusivity of a model hydrophilic drug, Rhodamine B (RhB; chemical structure shown in Figure 6) across the permeable lamellar phase formed between solutions of bile salt and chitosan, and how the diffusivity of the model drug across the bile salt−chitosan interface is affected by changes in temperature and salt concentration.

Babak et al. have previously shown the formation of capsules after dropwise addition of chitosan solution to a solution of sodium dodecyl sulfate (SDS), where the thickness of the gel bead, which purportedly possessed an ordered liquid-crystalline structure, grew over time.[46] Employing a similar approach, nanostructured spherical capsules (~0.3 cm in diameter) with reproducible surface area (~0.28 cm^2) were prepared by delivering a droplet of 4 wt % chitosan solution loaded with 1 mg/mL RhB dye into a stirred solution of 30 wt % STDC (1 mL in 2 mL glass vial) via a 25G syringe. The liquid-crystalline structure formed within the "outer shell" was allowed to develop over time while maintained at 37 °C. Aliquots (200 μL) of the release medium (surfactant solution) were sampled at predetermined time points and replaced with 200 μL of fresh drug-free solution. For the systems tested with different stimuli, either the temperature was increased to 50 °C from 37 °C, or the salt-free surfactant solution was replaced with 4% NaCl solution and kept at 37 °C, after ca. 2.25 h. A schematic of the release experiment is illustrated in Figure 6.

2.2.5. Determination of Rhodamine B Concentration in Release Medium. Aliquots of the release medium (surfactant solution) were taken during the release study and diluted with 10% (v/v) acetic acid and loaded into a 96 well plate. The fluorescence intensity of Rhodamine B in solution was measured at 37 °C using an EnSpire Multimode Plate Reader (PerkinElmer, Singapore) with an excitation and emission wavelength of 554 and 627 nm, respectively. The concentration of dye released was quantified using a calibration curve of Rhodamine B in blank media (see Figure S.2−S4 in the Supporting Information).

2.2.6. In Vitro Release Data Analysis. To determine the apparent diffusion coefficient, D (cm^2/s), of Rhodamine B across the single-sided matrix, we plotted the quantity expressing the moles of drug released per unit area, Q (mol/cm^2), against the square root of time, $t^{1/2}$ ($s^{1/2}$). The gradient of the linear curve from this plot was determined, which allowed for the calculation of D by applying the Higuchi equation1[47]

$$Q = 2C_0\sqrt{\frac{Dt}{\pi}} \quad (1)$$

where C_0 is the initial concentration of drug in the capsule (mol/cm^3). As previous studies have shown that liquid-crystalline systems display diffusion-controlled release,[9−11] data were plotted as % RhB released versus time$^{1/2}$ (Figure 7). The Higuchi equation is based on Fickian diffusion, which allows for the direct comparison between the different release rates of the same drug from mesophases with different structures.[48]

3. RESULTS

3.1. Liquid Crystalline Nanostructure(s) Formed Across Bile Salt−Chitosan Interfaces. *3.1.1. Growth and Development of Nanostructure.* When approximately equal volumes of bile salt solution (sodium taurodeoxycholate) were contacted with the chitosan solution within a flat cell, an initial interface was created, with the initial position defined as the "point of origin". At the interface, a band exhibiting birefringence was observed under CPLM at room temperature (Figure 4B), which was later confirmed to be lamellar (L_α) phase by SAXS with a lattice parameter of ca. 32 Å (Bragg reflections at spacing ratios 1 and 2, Figure 2). Micellar phase was present within the bulk 30 wt % STDC solution (spanning from close to 0 to approximately 4 mm away from the point of origin), which was indicated by the broad hump at low q values in the scattering profiles shown in Figure 2. It should be noted that chitosan and many other polymeric solutions scatter X-rays very poorly and therefore their scattering is not easily resolved in the flat cell configuration. In these experiments, nanostructures were allowed to develop over the duration of ca. 1 week, after which the L_α phase had grown predominantly toward the bulk chitosan side with the peaks slightly shifted to lower q ($Å^{-1}$) values. This change in the absolute position of the Bragg peaks relates to differences in the distance between repeating units within the liquid crystal nanostructure, i.e., its internal dimensions, which will be discussed later.

The effect of chitosan concentration on the kinetics of L_α phase formation was also investigated after ca. 1 week (Figure 3). At low polymer concentrations (1−2 wt %), L_α phase

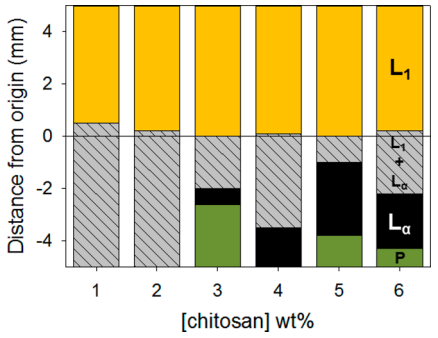

Figure 3. Effect of polymer concentration on the development of liquid-crystalline phases across the bile salt−chitosan interface after 1 week. Bar charts illustrate regions of bulk polymer (P, green), micellar phase (L_1, yellow), coexisting micellar and lamellar phases (L_1 + L_α, patterned gray), and only lamellar phase (L_α, black).

coexisted with micellar (L_1) phase, which spanned across the entire region previously occupied by chitosan solution at time zero. At higher concentrations (3−6 wt %), a distinct area comprised of only L_α phase arose in between the region of coexisting L_1 and L_α phases and the bulk polymer solution. As the latter concentration range of chitosan clearly demonstrated distinct sections in the flat cells where only lamellar phase was present, and for ease in handling and preparation in sample cells, the bile salt−chitosan composition selected for further studies comprised of 30 wt % STDC and 4 wt % chitosan.

3.1.2. Effect of Temperature and Salt Concentration on Lamellar Phase. Following the identification of lamellar phase formed in systems containing solutions of bile salt and chitosan, the structural integrity of the lamellar phase was examined in response to temperature and salt concentration. The influence of temperature is expected to probe the nature of the hydrophobic interactions between the bile salt surfaces. In the 30 wt % STDC:4 wt % chitosan system, micelles coexisted with L_α phase at room temperature. During the temperature scan, scattering indicative of lamellar phase persisted up until ca. 45 °C, above which the highly ordered structure disappeared. Images taken of the sample under CPLM-coupled with a hot stage were in agreement with SAXS data (Figure 4A), where the intensity of the birefringent band at the surfactant−polymer interface decreased with increasing temperature (Figure 4B).

The electrostatic interactions between the oppositely charged species were probed by introducing a salt solution containing 4% NaCl to the nanostructure formed at the interface. The amount of lamellar phase formed in the bile salt−chitosan system was found to decrease upon exposure to salt solution,

dx.doi.org/10.1021/am502192t | ACS Appl. Mater. Interfaces XXXX, XXX, XXX−XXX

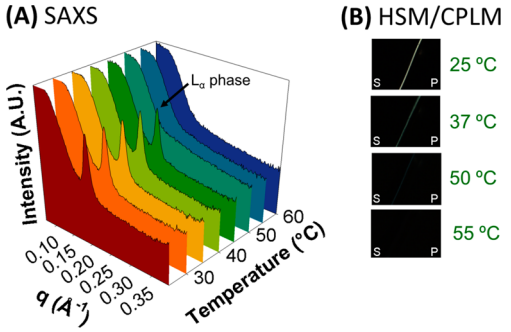

Figure 4. Effect of temperature on the structural integrity of lamellar phase formed between solutions of 4 wt % chitosan and 30 wt % STDC. (A) Waterfall plot of SAXS scattering profiles obtained for the system when exposed to heating from 25 to 60 °C at 5 °C increments. (B) Images taken of the sample under a crossed-polarizing light microscope (CPLM) fitted with a hot-stage (HSM), illustrating the disappearance of birefringence at the surfactant−polymer interface above 50 °C.

which was evident in a decrease in the scattering intensity of the first Bragg reflection peak and a blurred appearance of the band exhibiting birefringence at the surfactant−polymer interface under crossed-polarizers (Figure 5).

3.1.2. Liquid Crystalline Nanostructures Formed Across SDS−polyDADMAC Interfaces. For the purpose of comparison, the often studied oppositely charged polydiallyldimethylammonium chloride (polyDADMAC) and sodium dodecyl sulfate (SDS) was also investigated. Upon contact of a 20 wt % SDS solution with 20 wt % polyDADMAC solution, a hexagonal phase was found to grow at the interface, which preferentially developed toward the bulk surfactant region after a week (see Figure S2 in the Supporting Information). The nanostructure was shown to be temperature-stable (see Figure S3 in the Supporting Information) with no significant change in its lattice parameter (~43 Å) when heated (see Figure S3 in the Supporting Information), whereas the addition of salt lead to a decrease in the SAXS peak intensity along with a reduction in the width over which the hexagonal phase spanned across the SDS−polyDADMAC interface (see Figure S4 in the Supporting Information).

3.3. In Vitro Release Studies. Having established that the lamellar nanostructure is destabilized with heating to above 45 °C, or an increase in salt concentration, it was of interest to determine whether the bile salt−chitosan or SDS−polyDADMAC system may be useful as responsive liquid-crystalline drug delivery systems. This concept was examined by determining the rate of diffusion of a model hydrophilic drug, Rhodamine B (RhB), from within capsules, possessing the self-assembled structure in the wall and how the diffusion is responsive to temperature and salt stimuli.

Initially, when the capsules were created in surfactant solution at ca. 37 °C, the rate of Rhodamine B release from inside the capsule into the release medium displayed a slow diffusion-controlled process, as illustrated by a linear increase in release in Figure 7. After ca. 2.25 h, the temperature of a set of triplicate samples was elevated to ca. 50 °C, indicated by the arrow, whereupon a dramatic increase in the gradient of the release curve was observed. Similarly, when the bile salt solution was replaced with 4% NaCl solution for a different set of triplicate samples which were maintained at ca. 37 °C after ca. 2.25 h, a significant rise in the steepness of the % RhB released vs time$^{1/2}$ slope was also exhibited by the system in response to this stimulus (Figure 7).

The calculated diffusion coefficient (D) of Rhodamine B at the various experimental conditions (Table 1) studied were in agreement with the release profiles. Initially at ca. 37 °C, the rate of model drug release from the nanostructured capsules was ca. 0.07×10^{-6} cm^2 s^{-1}. When the temperature was elevated to ca. 50 °C after 2.25 h, the release of dye greatly increased, which was reflected in a 40 fold increase in D when compared to the system at ca. 37 °C. On the other hand, when the bile salt solution was replaced with a solution of 4% NaCl maintained at ca. 37 °C, the rate of diffusion of model drug across the liquid-crystalline matrix rose by 10-fold, a lower increase in comparison with the effect of temperature.

4. DISCUSSION

4.1. Formation of Lamellar Phase at Bile Salt−Chitosan Interfaces. Previous studies on the encapsulation capacity of proteins and adenoviral vectors in bile salt−chitosan microparticles are found in the literature.[49,50] The temperature dependent binding process experienced by these oppositely charged materials have also been described.[51] However, the mesophase-containing complexes formed upon contact between solutions of bile salt and chitosan have not been structurally characterized by X-ray scattering to date.

From the SAXS studies, it was clear that a lamellar phase forms in this system (Figure 2). Interestingly, inspection of the sodium taurodeoxycholate−water binary phase diagram indicates the absence of L_α phase.[35,52] For this reason, it can be postulated that it is a specific interaction between the

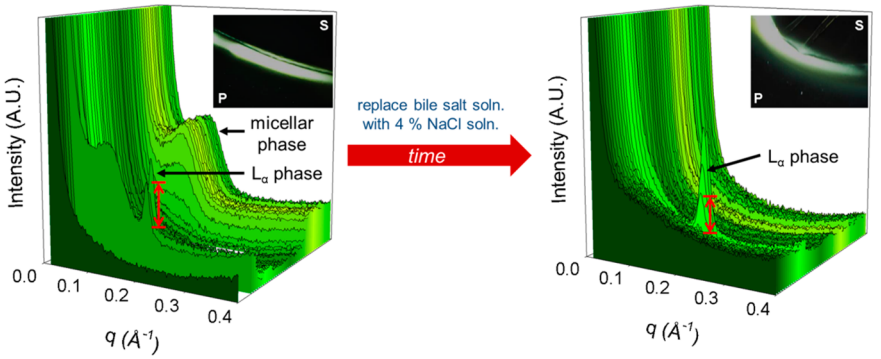

Figure 5. SAXS scattering profiles across the bile salt−chitosan interface (left) before and (right) after addition of 4% NaCl. Up−down arrows indicate changes in peak intensity, which correlates to the relative concentration of the lamellar phase formed. Insets: CPLM images.

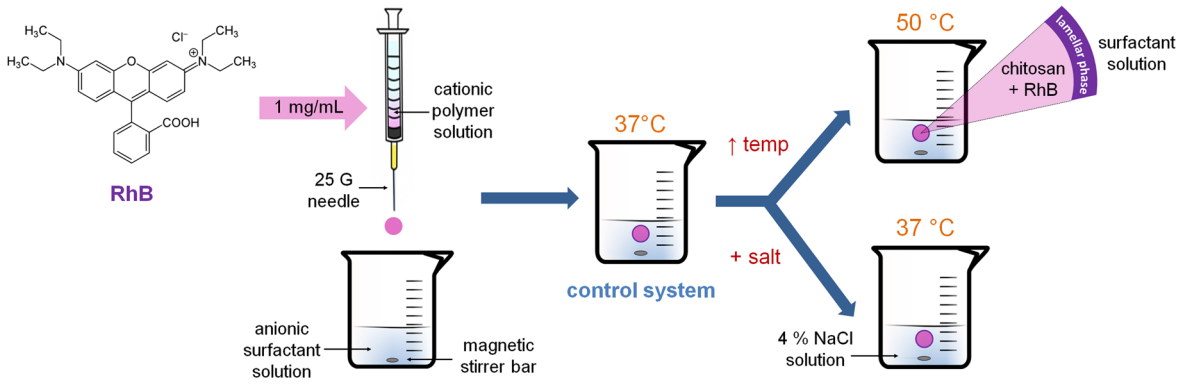

Figure 6. Approach for studying the effect temperature and salt has on the rate of model drug (Rhodamine B, RhB) release from nanostructured capsules.

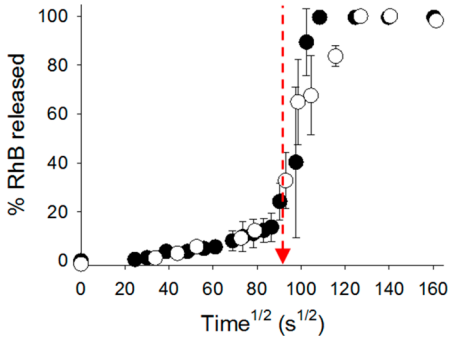

Figure 7. Cumulative % release profile of Rhodamine B (RhB) from bile salt−chitosan capsules, where the environmental temperature was increased from 37 to 50 °C (●) or when the bile salt solution was replaced with 4% NaCl solution at 37 °C (○), as indicated by the dashed arrow.

Table 1. Comparison of Rate of Diffusion of Rhodamine B (RhB) from Nanostructured Capsules Composed of Both Biologically and Industrially Relevant Materials at Varying Temperatures, from 37 °C (control) to 50 °C, and When Surfactant Solution Was Replaced with 4% NaCl Solution[a]

	diffusion coefficient of RhB ($\times 10^{-6}$ cm^2 s^{-1}) $n = 3$		
liquid-crystalline nanostructure	control (37 °C)	effect of temperature (50 °C)	effect of salt at 37 °C (4% NaCl solution)
lamellar phase	0.07 ± 0.1	3 ± 2	0.7
hexagonal phase	0.0002 ± 0.0001	0.0004 ± 0.0001	0.03 ± 0.07

[a]Literature value for the diffusion coefficient of RhB at 25 °C measured by a static imaging method in an aqueous solution was determined to be (4.27 ± 0.040) $\times 10^{-6}$ cm^2 s^{-1} (n = 13).

oppositely charged species that lead to the formation of lamellar phase. Bearing this in mind, it can be envisaged that with further understanding of the parameters that influence the way these surfactant and polymer molecules associate, nanomaterials can be generated with desired liquid-crystalline matrices possessing characteristic physicochemical properties and phase behavior in response to various environmental conditions.

The growth and development of L_α phase toward the bulk chitosan solution proved to be a peculiar unforeseen phenomenon (Figure 2). A possible explanation could be that the concentration gradient created between the opposing solutions drives the smaller surfactant molecules with greater mobility to traverse the interfacial region, and then to form new surfactant−polymer complex on the chitosan side. In contrast, the growth of hexagonal phase at the SDS−polyDADMAC interface was bidirectional, but projected predominantly toward the bulk surfactant solution (see Figure S2 in the Supporting Information). This observation contradicts the reason postulated for the behavior of the bile salt−chitosan system. Hence, the direction of growth will be the subject of future studies, where the ionic strength of both components of the surfactant−polymer systems will be investigated.

An increase in polymer concentration did not have an influence over the type of liquid-crystalline phase formed at the interface or the lattice parameter of the lamellar phase formed, but rather the extent to which L_α phase existed across the surfactant−polymer interface (Figure 3). At low polymer concentrations (1−2 wt %), L_α phase coexisted with micellar phase toward the bulk chitosan side of the interface. This suggests that the fewer polymer molecules present allowed for greater interfacial transport of the surfactant, and increased the interaction volume available for mesophase formation. At higher concentrations (3−6 wt %), L_α phase also developed, however the increased amount of polymer molecules in a given volume resulted in the slower growth of liquid-crystalline structures at the interface, due presumably to an increased density of the surfactant−polymer complex in this smaller volume. In other words, the movement of unbound surfactant molecules across this more dense/viscous interfacial region is impeded. In this instance, polymer encounters micelles (cmc of STDC of ∼3 mM by surface tension; ∼0.16 wt %)[53] at the interface between the two liquids, and the electrostatic interactions reorient the bile salt to form a bilayer based structure. Although the exact mechanism for this reorganization at short times is not yet understood, at very early time points birefringence is already observed on contact and lamellar phase scattering data at 2 h.

As discussed earlier, the hydrophobic and electrostatic interactions between the oppositely charged moieties play a crucial role on their geometric packing, which dictates the type of liquid-crystalline nanostructure that is formed.[54] Therefore, the phase behavior of the 30 wt % STDC:4 wt % chitosan system was studied against various experimental parameters. This particular surfactant−polymer composition was selected as it was shown to form a lamellar rich zone at the interface and where the concentration of chitosan was most easily handled.

dx.doi.org/10.1021/am502192t | ACS Appl. Mater. Interfaces XXXX, XXX, XXX−XXX

4.2. Structural Responsiveness of Lamellar Phase in Bile Salt−Chitosan Systems. The interfacial lamellar phase was found to be sensitive to both temperature and salt concentration. The most significant result that arose from the temperature scan was the complete loss of lamellar structure above ca. 45 °C. This suggests that the hydrophobic interactions are relatively weak, where only a small amount of energy input is required to increase the mobility of the associating molecules and cause a disruption to the packing within the liquid-crystalline nanostructure. In contrast, the hexagonal phase that is formed in the SDS−polyDADMAC system remained stable at high temperatures (see Figure S3 in the Supporting Information). The temperature at which the lamellar phase was lost is significant in the context of this system to act as a novel stimuli responsive drug delivery system. Drugs could be encapsulated within the capsule or the lamellar phase itself and the phase would remain stable at physiological temperature. Introducing heat via a heat pack, for example, to the site of administration would disrupt packing within the liquid-crystalline matrix, leading to the disintegration of the ordered structure and trigger the release of the therapeutic.

Addition of salt to the L_α phase resulted in the dissociation of the highly ordered nanostructure. Under crossed-polarizers, the band formed at the surfactant−polymer interface exhibiting birefringence became fragmented and decreased in intensity. This observation was reflected in a decrease in peak intensity and the distance over which L_α phase formed across the interface in the SAXS profile, which is indicative of a reduced amount of lamellar phase present. This was the result of a screening effect introduced between the opposite charges, where the strength of the electrostatic interactions is diminished in the presence of electrolyte; an effect that is well-known for oppositely charged surfactant and polymer systems in the literature.[22,24,26,30,39,55−58]

This demonstrates that changes in salt concentration, as well as temperature, can be employed to modulate the structural integrity of the lamellar phase and has potential for triggering release of therapeutic molecules from these complex matrices.

4.3. Triggered Release of Model Drug from Bile Salt−Chitosan Lamellar Capsules. The model hydrophilic drug, Rhodamine B (RhB), displayed a substantial increase in release across the lamellar phase formed in the bile salt−chitosan capsules when compared to that from the hexagonal phase forming SDS−polyDADMAC system. This supports the understanding that the liquid-crystalline structure acts as a diffusional barrier, controlling the rate of diffusion of small molecules across these liquid-crystalline systems.[9−11] It has been well-established for various lipid-based lyotropic liquid-crystalline systems that drugs are released much faster from inverse bicontinuous cubic phases as they possess continuous water channels, whereas release from hexagonal phases is much slower because of the tightly packed rodlike micellar structures.[9,10]

The distinct difference between the diffusion coefficient (D) calculated for the lamellar and hexagonal systems in this study at 37 °C could be related to the differences in rheology of the two systems. The lamellar phase, by virtue of the aqueous bilayer structure, appeared to be less viscous than the hexagonal phase formed in the SDS−polyDADMAC system. Therefore, the microrheology of the mesophases present at the surfactant−polymer interfaces likely plays an important role in controlling the diffusion of molecules across these intricate nanostructures; a subject that will be addressed in future microrheology studies.

Outcomes from the temperature scans correlated well with the in vitro release studies. Release of RhB from the L_α phase increased significantly at ca. 50 °C due to the loss of structure, whereas RhB released linearly versus square root of time from the hexagonal phase for the SDS−polyDADMAC system despite the increase in temperature. On the other hand, immersing the nanostructured-capsules into salt solution at ca. 37 °C did not induce as significant an effect on the rate of drug release, correlating with the modest effect of salt on structure in the CPLM and SAXS experiments. This perhaps may have depended on the time allowed for the liquid-crystalline phase to form at the surfactant−polymer interface before the stimulus was initiated, whereas a thicker "membrane barrier" would be produced when left for a longer duration, which in turn would require higher salt concentration and/or extended time for diffusion of molecules to occur to disturb the electrostatic interactions between charged species. Interestingly, the time-scale of drug release from lamellar phase (Figure 7) is consistent with the time oral dosage forms transit within the upper region of gastrointestinal tract (3−4 h),[59] whereas absorption of drug is at its highest owing to the large surface provided by the small intestine.[60] These findings provide a platform for these oppositely charged surfactant and polymer systems, bile salt−chitosan and SDS−polyDADMAC, to function as stimuli-responsive or sustained-release drug delivery systems, respectively.

5. CONCLUSION

This paper describes one of the first quantitative structural probes of these oppositely charged surfactant−polymer systems in relation to release, providing an initial proof of concept that temperature and salt concentration are potential parameters that may be exploited to modulate drug release from lamellar phase complexes formed between solutions of bile salt and chitosan. This is the first report of lamellar phase formation at bile salt−chitosan interfaces, where its growth and development is not only influenced by the apparent viscosity of bulk solutions, but also the characteristic physical properties exhibited by the complex formed. Therefore, controlling interfacial structural attributes in complex oppositely charged surfactant and polymer systems may provide an interesting route to tailored release nanomaterials. Future studies will involve exploring the effect of surfactant-to-polymer molar charge ratio on nanostructure formation, as well as performing release studies from dispersed nanoparticles.

■ ASSOCIATED CONTENT

Ⓢ Supporting Information

Details on the effect of bile salt concentration and pH on the formation of liquid-crystalline structure in the bile salt−chitosan system, calibration curve for Rhodamine B in water and acetic acid, lattice parameter vs temperature plot, and comparative studies on the SDS−polyDADMAC system. This material is available free of charge via the Internet at http://pubs.acs.org.

■ AUTHOR INFORMATION

Corresponding Author

*E-mail: ben.boyd@monash.edu.

Notes

The authors declare no competing financial interest.

■ ACKNOWLEDGMENTS

The authors acknowledge the Australian Institute of Nuclear Science and Engineering (ALNGRA11161), Procter & Gamble, and the Commonwealth Scientific and Industrial Research Organization (CSIRO) for funding this project. K.J.T. also thanks AINSE for support in the form of a Postgraduate Graduate Research Award. SAXS studies were conducted on the SAXS/WAXS beamline at the Australian Synchrotron, Victoria, Australia, as well as at the Bragg Institute at ANSTO. B.B. is the recipient of an ARC Future Fellowship.

■ REFERENCES

(1) Goddard, E.; Hannan, R. Polymer/Surfactant Interactions. *J. Am. Oil Chem. Soc.* **1977**, *54*, 561−566.
(2) Goddard, E. D.; Hannan, R. B. Cationic Polymer/Anionic Surfactant Interactions. *J. Colloid Interface Sci.* **1976**, *55*, 73−79.
(3) Wang, Y.; Hosta-Rigau, L.; Lomas, H.; Caruso, F. Nanostructured Polymer Assemblies Formed at Interfaces: Applications From Immobilization and Encapsulation to Stimuli-Responsive Release. *Phys. Chem. Chem. Phys.* **2011**, *13*, 4782−4801.
(4) Johnston, A. P. R.; Cortez, C.; Angelatos, A. S.; Caruso, F. Layer-by-layer Engineered Capsules and Their Applications. *Curr. Opin. Colloid Interface Sci.* **2006**, *11*, 203−209.
(5) Hössel; Dieing; Nörenberg; Pfau; Sander. Conditioning Polymers in Today's Shampoo Formulations − Efficacy, Mechanism and Test Methods. *Int. J. Cosmet. Sci.* **2000**, *22*, 1−10.
(6) Morán, M. C.; Miguel, M. G.; Lindman, B. Surfactant−DNA Gel Particles: Formation and Release Characteristics. *Biomacromolecules* **2007**, *8*, 3886−3892.
(7) Hsu, W.-L.; Li, Y.-C.; Chen, H.-L.; Liou, W.; Jeng, U. S.; Lin, H.-K.; Liu, W.-L.; Hsu, C.-S. Thermally-Induced Order−Order Transition of DNA−Cationic Surfactant Complexes. *Langmuir* **2006**, *22*, 7521−7527.
(8) Rosa, M. del Carmen Morán, M.; da Graça Miguel, M.; Lindman, B., The Association of DNA and Stable Catanionic Amino Acid-Based Vesicles. *Colloids Surf., A* **2007**, *301*, 361−375.
(9) Fong, W.-K.; Hanley, T.; Boyd, B. J. Stimuli Responsive Liquid Crystals Provide 'On-Demand' Drug Delivery in Vitro and in Vivo. *J. Controlled Release* **2009**, *135*, 218−226.
(10) Phan, S.; Fong, W.-K.; Kirby, N.; Hanley, T.; Boyd, B. J. Evaluating the Link Between Self-Assembled Mesophase Structure and Drug Release. *Int. J. Pharm.* **2011**, *421*, 176−182.
(11) Lee, K. W. Y.; Nguyen, T.-H.; Hanley, T.; Boyd, B. J. Nanostructure of Liquid Crystalline Matrix Determines In Vitro Sustained Release and In Vivo Oral Absorption Kinetics for Hydrophilic Model Drugs. *Int. J. Pharm.* **2009**, *365*, 190−199.
(12) Harada, A.; Nozakura, S.-i. Formation of Organized Structures in Systems of Polyelectrolyte-Ionic Surfactants. *Polymer Bull.* **1984**, *11*, 175−178.
(13) Nizri, G.; Magdassi, S.; Schmidt, J.; Cohen, Y.; Talmon, Y. Microstructural Characterization of Micro- and Nanoparticles Formed by Polymer−Surfactant Interactions. *Langmuir* **2004**, *20*, 4380−4385.
(14) Yeh, F.; Sokolov, E. L.; Khokhlov, A. R.; Chu, B. Nanoscale Supramolecular Structures in the Gels of Poly-(Diallyldimethylammonium Chloride) Interacting with Sodium Dodecyl Sulfate. *J. Am. Chem. Soc.* **1996**, *118*, 6615−6618.
(15) Svensson, A.; Norrman, J.; Piculell, L. Phase Behavior of Polyion−Surfactant Ion Complex Salts: Effects of Surfactant Chain Length and Polyion Length. *J. Phys. Chem. B* **2006**, *110*, 10332−10340.
(16) Thalberg, K.; Lindman, B.; Karlstroem, G. Phase Behavior of Systems of Cationic Surfactant and Anionic Polyelectrolyte: Influence of Surfactant Chain Length and Polyelectrolyte Molecular Weight. *J. Phys. Chem.* **1991**, *95*, 3370−3376.
(17) Chu, B.; Yeh, F.; Sokolov, E. L.; Starodoubtsev, S. G.; Khokhlov, A. R. Interaction of Slightly Cross-Linked Gels of Poly-(diallyldimethylammonium chloride) with Surfactants. *Macromolecules* **1995**, *28*, 8447−8449.
(18) Chronakis, I. S.; Alexandridis, P. Rheological Properties of Oppositely Charged Polyelectrolyte−Surfactant Mixtures: Effect of Polymer Molecular Weight and Surfactant Architecture. *Macromolecules* **2001**, *34*, 5005−5018.
(19) Zhou, S.; Xu, C.; Wang, J.; Golas, P.; Batteas, J.; Kreeger, L. Phase Behavior of Cationic Hydroxyethyl Cellulose−Sodium Dodecyl Sulfate Mixtures: Effects of Molecular Weight and Ethylene Oxide Side Chain Length of Polymers. *Langmuir* **2004**, *20*, 8482−8489.
(20) Zhou, S.; Burger, C.; Yeh, F.; Chu, B. Charge Density Effect of Polyelectrolyte Chains on the Nanostructures of Polyelectrolyte−Surfactant Complexes. *Macromolecules* **1998**, *31*, 8157−8163.
(21) Kogej, K.; Theunissen, E.; Reynaers, H. Effect of Polyion Charge Density on the Morphology of Nanostructures in Polyelectrolyte−Surfactant Complexes. *Langmuir* **2002**, *18*, 8799−8805.
(22) Starodubtsev, S. G.; Dembo, A. T.; Dembo, K. A. Effect of Polymer Charge Density and Ionic Strength on the Formation of Complexes Between Sodium Arylamido-2-methyl-1-propane-sulfonate-co-acrylamide Gels and Cetylpyridinium Chloride. *Langmuir* **2004**, *20*, 6599−6604.
(23) Loyen, K.; Iliopoulos, I.; Audebert, R.; Olsson, U. Reversible Thermal Gelation in Polymer/Surfactant Systems. Control of the Gelation Temperature. *Langmuir* **1995**, *11*, 1053−1056.
(24) Thongngam, M.; McClements, D. J. Influence of pH, Ionic Strength, and Temperature on Self-Association and Interactions of Sodium Dodecyl Sulfate in the Absence and Presence of Chitosan. *Langmuir* **2004**, *21*, 79−86.
(25) Sokolov, E.; Yeh, F.; Khokhlov, A.; Grinberg, V. Y.; Chu, B. Nanostructure Formation in Polyelectrolyte−Surfactant Complexes. *J. Phys. Chem. B* **1998**, *102*, 7091−7098.
(26) Merta, J.; Torkkeli, M.; Ikonen, T.; Serimaa, R.; Stenius, P. Structure of Cationic Starch (CS)/Anionic Surfactant Complexes Studied by Small-Angle X-ray Scattering (SAXS). *Macromolecules* **2001**, *34*, 2937−2946.
(27) Janiak, J.; Bayati, S.; Galantini, L.; Pavel, N. V.; Schillén, K. Nanoparticles with a Bicontinuous Cubic Internal Structure Formed by Cationic and Non-ionic Surfactants and an Anionic Polyelectrolyte. *Langmuir* **2012**, *28*, 16536−16546.
(28) Alatorre-Meda, M.; Taboada, P.; Sabín, J.; Krajewska, B.; Varela, L. M.; Rodríguez, J. R. DNA−Chitosan Complexation: A Dynamic Light Scattering Study. *Colloids Surf., A* **2009**, *339*, 145−152.
(29) Bronich, T. K.; Nehls, A.; Eisenberg, A.; Kabanov, V. A.; Kabanov, A. V. Novel Drug Delivery Systems Based on the Complexes of Block Ionomers and Surfactants of Opposite Charge. *Colloids Surf., B* **1999**, *16*, 243−251.
(30) Leonard, M. J.; Strey, H. H. Phase Diagrams of Stoichiometric Polyelectrolyte−Surfactant Complexes. *Macromolecules* **2003**, *36*, 9549−9558.
(31) Bilalov, A.; Olsson, U.; Lindman, B. DNA-Lipid Self-Assembly: Phase Behavior and Phase Structures of a DNA-Surfactant Complex Mixed with Lecithin and Water. *Soft Matter* **2011**, *7*, 730−742.
(32) Miguel, M. G.; Pais, A. A. C. C.; Dias, R. S.; Leal, C. amp; x; lia; Rosa, M.; Lindman, B., DNA−Cationic Amphiphile Interactions. *Colloid Surface Physicochem Eng. Aspect* **2003**, *228*, 43−55.
(33) Amar-Yuli, I.; Adamcik, J.; Blau, S.; Aserin, A.; Garti, N.; Mezzenga, R. Controlled Embedment and Release of DNA From Lipidic Reverse Columnar Hexagonal Mesophases. *Soft Matter* **2011**, *7*, 8162−8168.
(34) Admirand, W. H.; Small, D. M. The Physicochemical Basis of Cholesterol Gallstone Formation in Man. *J. Clin. Investig.* **1968**, *47*, 1043−1052.
(35) Marques, E. F.; Edlund, H.; La Mesa, C.; Khan, A. Liquid Crystals and Phase Equilibria Binary Bile Salt-Water Systems. *Langmuir* **2000**, *16*, 5178−5186.
(36) Hirano, S.; Seino, H.; Akiyama, Y.; Nonaka, I., Chitosan: A Biocompatible Material for Oral and Intravenous Administrations. In

Progress in Biomedical Polymers; Gebelein, C., Dunn, R., Eds.; Springer: New York, 1990; Chapter 28, pp 283−290.
(37) Hoogstraate, J. A. J.; Wertz, P. W. Drug Delivery via the Buccal Mucosa. *Pharm. Sci. Technol. Today* **1998**, *1*, 309−316.
(38) Harris, D.; Robinson, J. R. Drug Delivery via the Mucous Membranes of the Oral Cavity. *J. Pharm. Sci.* **1992**, *81*, 1−10.
(39) Mironov, A. V.; Starodoubtsev, S. G.; Khokhlov, A. R.; Dembo, A. T.; Dembo, K. A. Effect of Chemical Nature of 1,1-Salt on Structure of Polyelectrolyte Gel−Surfactant Complexes. *J. Phys. Chem. B* **2001**, *105*, 5612−5617.
(40) Sokolov, E. L.; Yeh, F.; Khokhlov, A.; Chu, B. Nanoscale Supramolecular Ordering in Gel−Surfactant Complexes: Sodium Alkyl Sulfates in Poly(diallyldimethylammonium Chloride). *Langmuir* **1996**, *12*, 6229−6234.
(41) Bakeev, K. N.; Shu, Y. M.; Zezin, A. B.; Kabanov, V. A.; Lezov, A. V.; Mel'nikov, A. B.; Kolomiets, I. P.; Rjumtsev, E. I.; MacKnight, W. J. Structure and Properties of Polyelectrolyte−Surfactant Nonstoichiometric Complexes in Low-Polarity Solvents. *Macromolecules* **1996**, *29*, 1320−1325.
(42) Tangso, K. J.; Fong, W.-K.; Darwish, T.; Kirby, N.; Boyd, B. J.; Hanley, T. L. Novel Spiropyran Amphiphiles and Their Application as Light-Responsive Liquid Crystalline Components. *J. Phys. Chem. B* **2013**, *117*, 10203−10210.
(43) Rosevear, F. B. The Microscopy of the Liquid Crystalline Neat and Middle Phases of Soaps and Synthetic Detergents. *J. Am. Oil Chem. Soc.* **1954**, *31*, 628−639.
(44) Kirby, N. M.; Mudie, S. T.; Hawley, A. M.; Cookson, D. J.; Mertens, H. D. T.; Cowieson, N.; Samardzic-Boban, V. A Low-Background-Intensity Focusing Small-Angle X-ray Scattering Undulator Beamline. *J. Appl. Crystallogr.* **2013**, *46*, 1670−1680.
(45) Hyde, S. *Handbook of Appled Surface and Colloid Chemistry*; John Wiley & Sons: 2001; p 299−332.
(46) Babak, V. G.; Merkovich, E. A.; Desbrières, J.; Rinaudo, M. Formation of an Ordered Nanostructure in Surfactant-Polyelectrolyte Complexes Formed by Interfacial Diffusion. *Polym. Bull.* **2000**, *45*, 77−81.
(47) Higuchi, W. I. Diffusional Models Useful in Biopharmaceutics. Drug Release Rate Processes. *J. Pharm. Sci.* **1967**, *56*, 315−324.
(48) Zabara, A.; Negrini, R.; Baumann, P.; Onaca-Fischer, O.; Mezzenga, R. Reconstitution of OmpF membrane Protein on Bended Lipid Bilayers: Perforated Hexagonal Mesophases. *ChemComm* **2014**, *50*, 2642−2645.
(49) Lameiro, M. H.; Malpique, R.; Silva, A. C.; Alves, P. M.; Melo, E. Encapsulation of Adenoviral Vectors into Chitosan−Bile Salt Microparticles for Mucosal Vaccination. *J. Biotechnol.* **2006**, *126*, 152−162.
(50) Lameiro, M. H.; Lopes, A.; Martins, L. O.; Alves, P. M.; Melo, E. Incorporation of a Model Protein into Chitosan−Bile Salt Microparticles. *Int. J. Pharm.* **2006**, *312*, 119−130.
(51) Thongngam, M.; McClements, D. J. Isothermal Titration Calorimetry Study of the Interactions Between Chitosan and a Bile Salt (Sodium Taurocholate). *Food Hydrocolloids* **2005**, *19*, 813−819.
(52) Youssry, M.; Coppola, L.; Furia, E.; Oliviero, C.; Nicotera, I. A New Physicochemical Characterization of Sodium Taurodeoxycholate/Water System. *Phys. Chem. Chem. Phys.* **2008**, *10*, 6880−6889.
(53) Kratohvil, J. P.; DelliColli, H. T. Micellar Properties of Bile Salts. Sodium Taurodeoxycholate and Sodium Glycodeoxycholate. *Can. J. Biochem.* **1968**, *46*, 945−952.
(54) Israelachvili, J. N.; Mitchell, D. J.; Ninham, B. W. Theory of Self-Assembly of Hydrocarbon Amphiphiles into Micelles and Bilayers. *J. Chem. Soc., Faraday Trans. 2* **1976**, *72*, 1525−1568.
(55) Thalberg, K.; Lindman, B.; Karlstroem, G. Phase Behavior of a System of Cationic Surfactant and Anionic Polyelectrolyte: The Effect of Salt. *J. Phys. Chem.* **1991**, *95*, 6004−6011.
(56) Abraham, A.; Mezei, A.; Meszaros, R. The Effect of Salt on the Association Between Linear Cationic Polyelectrolytes and Sodium Dodecyl Sulfate. *Soft Matter* **2009**, *5*, 3718−3726.
(57) Pojják, K.; Bertalanits, E.; Mészáros, R. B. Effect of Salt on the Equilibrium and Nonequilibrium Features of Polyelectrolyte/Surfactant Association. *Langmuir* **2011**, *27*, 9139−9147.
(58) Mironov, A. V.; Starodoubtsev, S. G.; Khokhlov, A. R.; Dembo, A. T.; Yakunin, A. N. Ordered Nonstoichiometric Polymer Gel−Surfactant Complexes in Aqueous Medium with High Ionic Strength. *Macromolecules* **1998**, *31*, 7698−7705.
(59) Yu, L. X.; Crison, J. R.; Amidon, G. L. Compartmental Transit and Dispersion Model Analysis of Small Intestinal Transit Flow in Humans. *Int. J. Pharm.* **1996**, *140*, 111−118.
(60) Ritschel, W. A. Targeting in the Gastrointestinal Tract: New Approaches. *Methods Find. Exp. Clin. Pharmacol.* **1991**, *13*, 313−336.
(61) Squier, C. A.; Hall, B. K. The Permeability of Skin and Oral Mucosa to Water and Horseradish Peroxidase as Related to the Thickness of the Permeability Barrier. *J. Investig. Dermatol.* **1985**, *84*, 176−179.